Transport properties of electrons in water vapor

K. F. Ness and R. E. Robson

Physics Department, James Cook University of North Queensland, Townsville, Queensland, 4811, Australia

(Received 8 December 1987)

Accurate values of transport properties of electrons in water vapor at room temperature are calculated, over a wide range of E/n_0 values, from a numerical solution of Boltzmann's equation via the momentum method introduced earlier [Phys. Rev. A **33**, 2068 (1986); **34**, 2185 (1986)]. The dominant features of the E/n_0 dependence are explained using the approximate momentum-transfer theory. For the electron–water-vapor rotational interactions the Born-approximation cross sections of Y. Itikawa [J. Phys. Soc. Jpn. **32**, 217 (1972)] have been used to obtain satisfactory agreement with experiment.

I. INTRODUCTION

The transport properties of electron swarms in water vapor are not only of considerable practical significance for a wide range of fields, e.g., studies of insulation properties of air, magnetohydrodynamics (MHD) plasmas, atmospheric and space physics, but have also an intrinsic interest because of their striking variation[1-5] with E/n_0 (the ratio of applied electrostatic field to the number density of water molecules). As is well known, this E/n_0 dependence is a reflection of microscopic properties, such as scattering cross sections, and indeed, one of the most useful applications of swarm experiment data is in the determination of these cross sections. Unfortunately, swarm data for electrons in water vapor are incomplete and the subject of some controversy.[1] Moreover, it is only in the last few years that an accurate transport theory has been developed,[6,7] suitable for use in conjunction with swarm data. Previous theoretical treatments[8] have relied on the so-called two-term approximation[5] of the electron velocity distribution function and/or have neglected important correction factors[6] which arise because of nonconservative collisions (attachment, ionization, etc.). We therefore agree with Gallagher et al.[1] that the calculation of transport properties of electrons in water vapor is a matter of priority, all the more so because of the recent highly accurate measurements of transverse diffusion coefficient at low E/n_0 by Elford,[4] and this article is directed towards that end.

In Sec. II we apply the ideas of Ref. 9, in conjunction with model cross sections, to provide a semiquantitative description of electrons in water vapor. The aim there is to understand the unusual E/n_0 dependence of the transport coefficients, with physical considerations to the fore.

In Sec. III we present values of transport coefficients obtained by the "multiterm" solution of Boltzmann's equation using the so-called method of moments.[6] Here we rely on cross sections derived from both swarm and beam experiments[2,10,11] and from *ab initio* quantum-mechanical calculations.[12-16] Further cross-section data appear in Refs. 17 and 18, while Ref. 19 contains information on optical line strengths necessary for computation of cross sections involving excitation of rotational modes. We compare our calculations with swarm experiments, but have not attempted to adjust cross sections to fit the swarm data. Lowke and Parker[8] have also solved Boltzmann's equation for electrons in water vapor using the two-term approximation and an unpublished cross-section data set of Cohen and Phelps. Their calculations agree qualitatively with ours, but no direct comparison is made since we use a different set of cross sections. We also comment on the accuracy of the two-term approximation for electrons in water vapor.

II. MOMENTUM-TRANSFER APPROXIMATION

A. Summary of relevant equations

If $m/m_0 \ll 1$, Eqs. (5.18) of Ref. 9 give the following equations for average velocity w and mean energy ε of the electron swarm:

$$w = \frac{eE}{m \nu_m} , \tag{1}$$

$$\varepsilon = \tfrac{3}{2}kT_0 + \tfrac{1}{2}m_0 w^2 - \Omega - \tfrac{2}{3}\varepsilon^2 (dv^*/d\varepsilon)/\nu_e(\varepsilon) , \tag{2}$$

where m and e are the electron mass and charge, respectively, m_0 and T_0 are the neutral-gas molecular mass and temperature, respectively, k is Boltzmann's constant,

$$\Omega = \sum_\alpha \epsilon_\alpha (\bar{v}_\alpha - \bar{v}_\alpha)/\nu_e , \tag{3}$$

and

$$\nu_e \equiv \frac{2m}{m_0} \nu_m$$

is the average energy-transfer collision frequency. The average momentum-transfer collision frequency is given by

$$\nu_m(\varepsilon) = n_0 \left[\frac{2\varepsilon}{m} \right]^{1/2} \sigma_m(\varepsilon) , \tag{4}$$

where $\sigma_m(\varepsilon)$ is the average momentum-transfer cross section. Likewise, the quantity

$$\vec{v}_\alpha(\varepsilon) = x_\alpha n_0 \left[\frac{2\varepsilon}{m}\right]^{1/2} \sigma_\alpha(\varepsilon) \quad (\alpha = 1, 2, 3, \ldots) \tag{5}$$

denotes the average frequency of collisions inducing inelastic process α, characterized by the cross section σ_α and threshold energy ϵ_α. Molecular abundance in the initial state is denoted by x_α. Superelastic collisions are described by the collision frequency

$$\vec{v}_\alpha(\varepsilon) \approx \vec{v}_\alpha(\varepsilon) \exp\left[-\epsilon_\alpha \left[\frac{1}{kT_0} - \frac{\frac{3}{2}}{\varepsilon}\right]\right], \tag{6}$$

an expression which is derived from considerations of microscopic reversibility and which is exact for a Maxwellian energy distribution.

The average particle loss rate v^* can be similarly expressed in terms of an appropriate cross section σ^*, but care must be taken to represent v^* realistically in cases where σ^* varies sharply near its threshold.[20] We shall postpone discussion of this point until Sec. II B.

Equations (1) and (2) are to be solved for w and ε as functions of E/n_0 and T_0, for a specified model of interaction $\sigma_m, \sigma^*, \sigma_\alpha$ $(\alpha = 1, 2, \ldots)$. Drift velocity W and transverse and longitudinal diffusion coefficients $D_\perp$ and $D_\parallel$ respectively, can then be found from Eqs. (5.31)–(5.33) of Ref. 9. If it is assumed that the distribution of electron velocities is very nearly isotropic,

$$\varepsilon \approx \tfrac{3}{2} kT_\parallel \approx \tfrac{3}{2} kT_\perp ,$$

where $T_\perp$ and $T_\parallel$ denote the electron temperature perpendicular and parallel to the field, respectively, then the expressions for transport coefficients simplify to

$$W = w \left[1 - \frac{2\varepsilon}{3ew} \frac{dk^*}{d(E/n_0)}\right], \tag{7}$$

$$\frac{D_\perp}{K} = \frac{2\varepsilon}{3e} \left[1 + \frac{\varepsilon}{3eW} \frac{dk^*}{d(E/n_0)}\right], \tag{8}$$

and

$$\frac{D_\parallel}{K} = \frac{2\varepsilon}{3e} \left[1 + \frac{d \ln K}{d \ln(E/n_0)} + \frac{\varepsilon}{3eKn_0} \frac{d^2 k^*}{d(E/n_0)^2}\right], \tag{9}$$

respectively, where

$$k^*(E/n_0) = \frac{1}{n_0} v^*[\varepsilon(E/n_0)] \tag{10}$$

is the reaction rate coefficient and

$$K \equiv W/E$$

is the mobility.

B. Simplified model of electron–water-molecule interaction

It is consistent with the spirit of momentum-transfer theory to employ model cross sections in order to facilitate analytic solution of our equations wherever possible. More realistic, tabulated cross sections are employed in Sec. III, where transport coefficients obtained from accurate solution of Boltzmann's equation are presented.

The dominating influence, generally speaking, is the intrinsic dipole moment of the water-vapor molecule. The momentum-transfer cross section for a point-charge–dipole interaction is known[14] to be inversely proportional to energy and we therefore write

$$\sigma_m(\epsilon) = s_m/\epsilon , \tag{11}$$

where s_m is a constant, whose value may be taken as

$$s_m \approx 30 \text{ eV Å}^2$$

for the purposes of this section and ϵ denotes the relative energy of collision.

At energies greater than or equal to several eV, σ_m is known to rise with energy.[2,16] However, for the range of parameters considered here, (11) is a reasonable approximation, and in any case, there is by no means general agreement on the form of σ_m.[18] This type of energy dependence leads to unusual, if not spectacular, properties of transport coefficients.

The Born approximation has been used by Itikawa[12] and Crawford[15] to calculate inelastic cross sections leading to excitation of rotational states in the water molecule. The dipole interaction again dominates here, and the total cross section $\sigma_\alpha^{(rot)} \equiv \sigma_{0,\alpha}^{(rot)}$ for rotational inelastic process α is given by Eqs. (44) and (45a). For $\epsilon \gg \epsilon_\alpha^{(rot)}$, $\sigma_\alpha^{(rot)}$ is effectively inversely proportional to energy. Threshold energies are quite low, ranging from 2.3 meV to a few tens of meV for the most significant transitions. Inelastic collisions of this type therefore strongly influence swarm properties for near thermal energies ~ 38 meV.

On the other hand, the threshold for excitation of vibrational modes lie at much higher energies: 0.198 eV for the bending mode and 0.453 and 0.466 eV for the symmetric and asymmetric stretching modes, respectively. Itikawa's investigations[13] using the Born approximation indicate that, unlike rotational excitation, dipole interaction is by no means dominant and that in fact quadrupole interaction, characterized by an essentially constant cross section, gives the greatest contribution to the total cross section at higher energies. However, Seng and Linder[10] demonstrated experimentally that strong resonances, unaccounted for in the Born approximation, lead to cross sections several times that prediced by Itikawa. Dependence upon energy is particularly sharp just above threshold, but for higher energies it introduces no great error into the calculations to assume constant cross sections, i.e.,

$$\sigma_\alpha^{(vib)}(\epsilon) \approx \text{const}, \quad \epsilon \gg \epsilon_\alpha^{(vib)} . \tag{12}$$

Dissociative attachment of a water molecule by electron impact has a threshold energy of 4.3 eV, but first becomes appreciable at ~ 6 eV and peaks at 6.4 eV (Ref. 17, Fig. 5). We are primarily interested in the subthreshold region and model attachment by a constant cross section

$$\sigma_a(\epsilon) = \begin{cases} \sigma_a, & \epsilon > \epsilon_a \\ 0, & \epsilon < \epsilon_a \end{cases}$$

where σ_a and ϵ_a denote the attachment cross section and threshold, respectively. Electronic excitation also be-

comes important in the neighborhood of the attachment threshold and we model this also by a constant, but much larger cross section, $\sigma^{(ex)}$, with threshold $\epsilon^{(ex)} = \epsilon_a$ (see Table I).

In the present investigation we work with $T_0 = 294$ K, so that $\epsilon^{(ex)}$ and $\epsilon_\alpha^{(vib)} \gg kT_0$. For the vibrational and electronic excitation processes we therefore set the molecular abundance of the lower state to 1. Henceforth x_α denotes the molecular abundance of the lower state for the rotational transitions only.

As explained in Ref. 20, it is sometimes desirable to incorporate a "smoothing factor" S in the expression for average collision frequency if the cross section varies rapidly near its threshold. This is certainly the case with most of the processes described above, but we dispense with this refinement for all but the electronic excitation and attachment processes, where we write for the respective rates

$$v^{(ex)}(\varepsilon) = n_0 \sqrt{2\varepsilon/m} \, \sigma^{(ex)} S(\xi)$$

and

$$v^*(\varepsilon) = n_0 \sqrt{2\varepsilon/m} \, \sigma_a S(\xi) \, ,$$

where[20]

$$S(\xi) = (1 + \xi)e^{-\xi} \tag{13}$$

and

$$\xi = 3\epsilon_a/2\varepsilon = 3\epsilon^{(ex)}/2\varepsilon \, .$$

Our equations contain the derivative

$$\frac{dv^*}{d\varepsilon} = \frac{n_0 \sqrt{2\varepsilon/m} \, \sigma_a}{2\varepsilon}(1 + \xi + 2\xi^2)e^{-\xi} \, . \tag{14}$$

The most important qualitative effect of the inclusion of S is to allow attachment for mean energies below ϵ_a.

Ionization becomes important at even higher energies and could be dealt with by inclusion of an additional term in Eqs. (2), (7), (8), and (9). This effect is studied only in connection with the solution of Boltzmann's equation (Sec. III) and its omission introduces no error into the present semiquantitative discussion.

C. Energy balance equation

Substitution of (11) into (4) yields

$$v_m(\varepsilon) = n_0 \left[\frac{2\varepsilon}{m} \right]^{1/2} \frac{s_m}{\varepsilon} \, ,$$

and substitution of this expression into (1) and (3) gives

TABLE I. Shows the values of parameters used to model vibrational, electronic excitation, and attachment processes.

Process	Threshold (eV)	Cross section (Å^2)
Vibration		
(i) Bending	0.198	0.2
(ii) Stretch	0.455	0.6
Electronic	6.0	1.0
Attachment	6.0	0.06

$$w = \left[\frac{\varepsilon}{2m} \right]^{1/2} \frac{eE}{s_m n_0} \tag{15}$$

and

$$\Omega = \Omega^{(rot)} + \varepsilon\omega^{(vib)} + \varepsilon\omega^{(ex)} \, , \tag{16}$$

respectively, where

$$\Omega^{(rot)} = \varepsilon \sum_\alpha \frac{x_\alpha \epsilon_\alpha^{(rot)} \sigma_a^{(rot)}}{2\frac{m}{m_0} s_m}(1 - \delta_\alpha^{(rot)}) \, , \tag{17}$$

$$\omega^{(vib)} = \sum_\alpha \frac{\epsilon_\alpha^{(vib)} \sigma_\alpha^{(vib)}}{2\frac{m}{m_0} s_m} \, , \tag{18a}$$

$$\omega^{(ex)} = \frac{\epsilon^{(ex)} \sigma^{(ex)} S(\xi)}{2\frac{m}{m_0} s_m} \, , \tag{18b}$$

and

$$\delta_\alpha^{(rot)} \equiv \exp\left[-\epsilon_\alpha^{(rot)} \left[\frac{1}{kT_0} - \frac{\frac{3}{2}}{\varepsilon} \right] \right] \, . \tag{19}$$

The latter quantity accounts for rotational deexcitation in superelastic collisions. The corresponding quantity for vibrations and electronic excitation is negligibly small since $\epsilon^{(ex)}, \epsilon_\alpha^{(vib)} \gg kT_0$ and has been omitted from (18). Substitution of (14), (15), and (16) into (2) then yields

$$\varepsilon = 3/2kT_0 + \varepsilon A(E/n_0)^2 - \Omega^{(rot)}$$

$$- \varepsilon\omega^{(vib)} - \varepsilon\omega^{(ex)} - \frac{\varepsilon^2}{\varepsilon^*}\chi\left[\frac{3\epsilon_a}{2\varepsilon} \right] \, , \tag{20}$$

where

$$A = \frac{m_0}{4m} \left[\frac{e}{s_m} \right]^2 = 9.18 \times 10^{-2} \text{ Td}^{-2} \, , \tag{21a}$$

with 1 Td $= 10^{-21}$ V m^2,

$$\varepsilon^* = \frac{6m}{m_0} \frac{s_m}{\sigma_a} = 9.078 \times 10^{-2} \text{ eV} \, , \tag{21b}$$

and

$$\chi(\xi) = (1 + \xi + 2\xi^2)e^{-\xi} \, . \tag{22}$$

To facilitate the analytic solution of (20), we assume that the most important transitions in rotational excitation are those for which $\epsilon_\alpha^{(rot)} < kT_0$ and hence by (19)

$$1 - \delta_\alpha^{(rot)} \approx \epsilon_\alpha^{(rot)} \left[\frac{1}{kT_0} - \frac{\frac{3}{2}}{\varepsilon} \right] \, . \tag{23}$$

Thus (17) becomes

$$\Omega^{(rot)} \approx \omega^{(rot)}(\varepsilon - \tfrac{3}{2}kT_0) \, , \tag{24}$$

where

$$\omega^{(rot)} = \sum_\alpha \frac{x_\alpha (\epsilon_\alpha^{(rot)})^2 \sigma_\alpha^{(rot)}(\varepsilon)}{2\frac{m}{m_0} s_m kT_0} \, . \tag{25}$$

The energy balance equation (20) can thus be written as

$$\frac{\varepsilon^2}{\varepsilon^*}\chi\left[\frac{3\varepsilon_a}{2\varepsilon}\right]+\varepsilon[1-A(E/n_0)^2+\omega^{(rot)}+\omega^{(vib)}+\omega^{(ex)}]=\tfrac{3}{2}kT_0(1+\omega^{(rot)})\ . \tag{26}$$

We consider solution of this equation in several different energy regimes:

1. Near thermal equilibrium

For sufficiently weak fields such that

$$\varepsilon\gtrsim\tfrac{3}{2}kT_0\ , \tag{27}$$

the parameter $\xi=3\epsilon_a/2\varepsilon$ is ~240 and both $S(\xi)$ of (13) and $\chi(\xi)$ of (22) are exceedingly small, i.e., electronic excitation and attachment are negligible. Equation (26) can then be written in the form

$$\varepsilon=\frac{\tfrac{3}{2}kT_0}{1-\left[\dfrac{E}{n_0f(\varepsilon)}\right]^2+B(\varepsilon)}\ , \tag{28}$$

where

$$f(\varepsilon)=\left[\frac{1+\omega^{(rot)}(\varepsilon)}{A}\right]^{1/2} \tag{29}$$

and

$$B(\varepsilon)=\frac{\omega^{(vib)}(\varepsilon)}{1+\omega^{(rot)}(\varepsilon)}\ . \tag{30}$$

Equation (28) can be solved by iteration. With an initial estimate $\varepsilon=\tfrac{3}{2}kT_0$ substituted in the right-hand side (rhs), we obtain as the first iterate

$$\varepsilon=\frac{\tfrac{3}{2}kT_0}{1-\left[\dfrac{e}{n_0f(\tfrac{3}{2}kT_0)}\right]^2}$$

$$\approx\tfrac{3}{2}kT_0\left[1+\left[\frac{E}{n_0f(\tfrac{3}{2}kT_0)}\right]^2+\cdots\right]\ , \tag{31}$$

where it has been assumed that

$$\omega^{(vib)}(\tfrac{3}{2}kT_0)\ll1$$

and therefore B has been neglected. Equation (31) is mathematically valid and consistent with the condition (27) if and only if

$$\frac{E}{n_0}<f(\tfrac{3}{2}kT_0)\ . \tag{32}$$

Equation (8) then gives (again neglecting attachment)

$$\frac{D_\perp}{K}=\frac{kT_0}{e}\left[1+\left[\frac{E}{n_0f(\tfrac{3}{2}kT_0)}\right]^2\right] \tag{33}$$

and comparison with the low-field $(E/n_0\leq26$ Td) data of Elford[4] at room temperature indicates that

$$f(\tfrac{3}{2}kT_0)\approx71\ \text{Td}\ . \tag{34}$$

For internal consistency, the above analysis should therefore be limited to $E/n_0\lesssim20$ Td.

The experimental value (34), when combined with (25) and (29), furnishes the following summational constraint on the rotational cross sections:

$$\sum_\alpha x_\alpha(\epsilon_\alpha^{(rot)})^2\sigma_\alpha^{(rot)}(\tfrac{3}{2}kT_0)\approx2.1\times10^{-2}\ (\text{eV Å})^2\ , \tag{35}$$

for $T_0=294$ K, where units of $\epsilon_\alpha^{(rot)}$ and σ_α are eV and Å^2, respectively.

It is interesting to note that if inelastic and attachment processes were absent, the electron swarm would "runaway." Taking $\omega^{(rot)}$, $\omega^{(vib)}$, $\omega^{(ex)}$, and χ all zero in (26), we find

$$\varepsilon=\frac{\tfrac{3}{2}kT_0}{1-A(E/n_0)^2}\ , \tag{36}$$

indicating an infinite singularity in ε (and therefore all other transport parameters) at a critical value of field

$$E/n_0=A^{-1/2}=3.3\ \text{Td}\ . \tag{37}$$

The origin of this effect can be traced directly to the nature of the energy dependence of σ_m, as shown in Eq. (11). The rotational processes only temporarily suppress the runaway of electrons in water vapor: It is the reactive and higher threshold inelastic process that ultimately quench the singularity. Nevertheless transport properties all show a steep rise over a certain narrow range of E/n_0 and this may be thought of as a "quasi-runaway" phenomenon generated by the rapidly falling nature of $\sigma_m(\varepsilon)$ with increasing ε. This is discussed further in Sec. III.

2. Intermediate fields

As E/n_0 is increased above 30 Td, ε begins to deviate significantly from $3/2kT_0$ although it may still lie well below the threshold ϵ_a for attachment and electronic excitation. If these processes are negligible, Eq. (28) is still applicable, and may be solved by iteration. It is interesting to speculate what would happen if attachment and electronic excitation were absent altogether, bearing in mind that $\omega^{(rot)}\to0$ and $\omega^{(vib)}\to$constant for sufficiently large ε. Let us assume that this situation prevails, so that (28) becomes

$$\varepsilon=\frac{\tfrac{3}{2}kT_0}{1+\omega^{(vib)}-A(E/n_0)^2} \tag{38}$$

and the mean energy exhibits a singularity for a critical value of field

$$E/n_0\left[\frac{1+\omega^{(vib)}}{A}\right]^{1/2}\approx43\ \text{Td}\ , \tag{39}$$

where the rhs has been evaluated using Table I and (18).

Comparison of (37) and (39) demonstrates that the effect of inelastic collisions is to displace the singularity to a higher field, not to eliminate it.

Although this potential runaway situation is ultimately quenched, transport properties do nevertheless exhibit a sharp increase in values for E/n_0 in the range 40–80 Td.[1-5] In view of the above discussion, we may label this behavior as quasirunaway.

If we now allow for attachment and electronic excitation and assume a mean energy sufficiently large so that $\omega^{(rot)}$ is negligible but nevertheless $\xi = 3\epsilon_a/2\epsilon$ is still large, then (26) becomes

$$\frac{9\epsilon_a^2}{2\tilde{\epsilon}^*}\exp\left[\frac{3\epsilon_a}{2\epsilon}\right] \approx \tfrac{3}{2}kT_0 - \epsilon[1+\omega^{(vib)} - A(E/n_0)^2] ,$$

where

$$\tilde{\epsilon}^* = 6\frac{m}{m_0}\frac{s_m}{\sigma_a+\sigma^{(ex)}}$$

$$\approx \frac{\sigma_a}{\sigma^{(ex)}}\epsilon^* = 5.45\times10^{-3} \text{ eV} .$$

When E/n_0 satisfies (39), the second term on the rhs vanishes and we find

$$\epsilon = \frac{\tfrac{3}{2}\epsilon_a}{\ln\left[\dfrac{3\epsilon_a^2}{\epsilon^*kT_0}\right]} = 0.662 \text{ eV} . \tag{40}$$

Small departures from (39) lead to quite different values of ϵ, such is the delicate nature of the balance between the tendency to runaway and the quenching effect.

There has been some discussion[1] in the literature as to the value of E/n_0 at which attachment becomes important. The above argument indicates that the onset of attachment is rapid, being induced by the quasirunaway effect over a relatively narrow range of E/n_0.

It is also of interest to estimate the explicit reactive correction term in Eq. (7). If we define

$$\delta_W = \frac{2\epsilon}{3ew}\frac{dk^*}{d(E/n_0)} = \frac{2\epsilon}{3ewn_0}\frac{dv^*d\epsilon}{d\epsilon\,d(E/n_0)}$$

then by (7) the ratio of measured drift velocity to average velocity is

$$\frac{W}{w} = 1-\delta_W , \tag{41a}$$

and for E/n_0 satisfying (39), we find

$$\delta_W = \frac{2\sigma_a}{\sigma^{(ex)}\ln\left[\dfrac{3\epsilon_a^2}{\tilde{\epsilon}^*kT_0}\right]} = 8.8\times10^{-3} . \tag{41b}$$

Corrections to diffusion coefficients, (8) and (9), are similarly small for this value of E/n_0. It is only at much higher fields that reactive terms become significant.

3. High fields

We do not wish to use simple model cross sections for the high-energy high-field range, for the actual cross sec-

tions are quite complicated (Figs. 1 and 2). Instead, for the sake of completeness, we give a qualitative discussion of transport coefficient behavior at high E/n_0 and leave the details for the numerical analysis of Sec. III.

At high E/n_0, we assume that ionization dominates attachment (Fig. 3) and hence in Eqs. (7), (8), and (9), k^* is negative, i.e.,

$$k^* = -k_i ,$$

where k_i denotes the ionization rate coefficient.

Referring to Fig. 3, it can be seen that the first derivative of k_i with respect to E/n_0 is positive and the second derivative is negative, i.e.,

$$\frac{dk^*}{d(E/n_0)} < 0 ,$$

$$\frac{d^2k^*}{d(E/n_0)^2} > 0 .$$

Hence, by Eqs. (7), (8), and (9), we have, respectively,

$$W > w ,$$

$$\frac{D_\perp}{K} < \frac{\mathcal{D}_\perp}{\mathcal{K}} ,$$

and

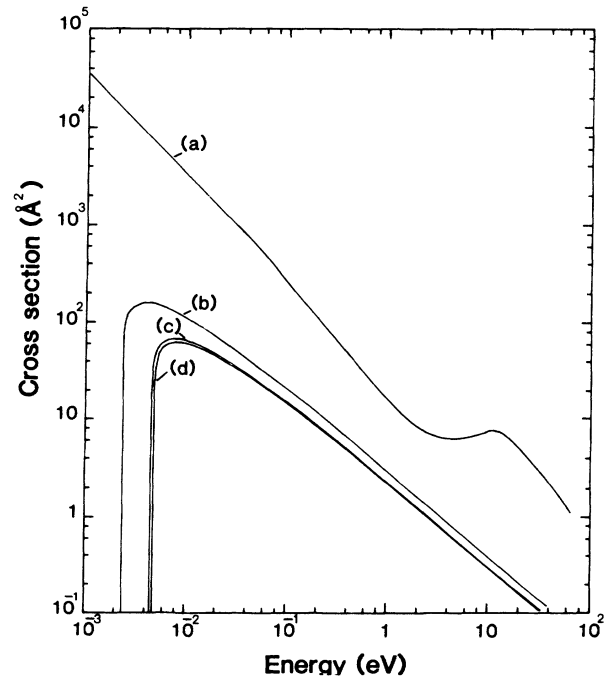$$\frac{D_\parallel}{K} > \frac{\mathcal{D}_\parallel}{\mathcal{K}} ,$$

FIG. 1. (a) Total momentum-transfer cross section for electrons in water vapor, from Pack et al. (Ref. 2) and Gianturco and Thompson (Ref. 16). (b)–(d) three largest total ($l = 0$) Itikawa (Ref. 12) rotational cross sections for electrons in water vapor weighted by the relative abundance of the lower level in the transition.

where

$$\mathcal{H} = w/E$$

and

$$\frac{\mathcal{D}_\perp}{\mathcal{H}} \equiv \frac{2\varepsilon}{3e} \,,$$

$$\frac{\mathcal{D}_\parallel}{\mathcal{H}} \equiv \frac{2\varepsilon}{3e} \left[1 + \frac{d\ln\mathcal{H}}{d\ln(E/n_0)} \right]$$

are transport quantities with explicit reactive effects excluded.[6] The above inequalities are in accord with calculations from the Boltzmann equation shown in Figs. 4–6, respectively.

III. BOLTZMANN ANALYSIS

A. Cross sections

In this section the Boltzmann equation describing the motion of electrons in water vapor is solved by using the moment method.[6] The collision cross sections used are shown in Figs. 1 and 2. For the total momentum-transfer cross section we combine the cross section of Pack,

FIG. 3. Ionization and attachment rate coefficients for electrons in water vapor as a function of E/n_0, $T_0 = 294$ K. The dashed section of the curve represents extrapolation based on partially converged moment solution. $1 \text{ Td} = 10^{-21} \text{ V m}^2$.
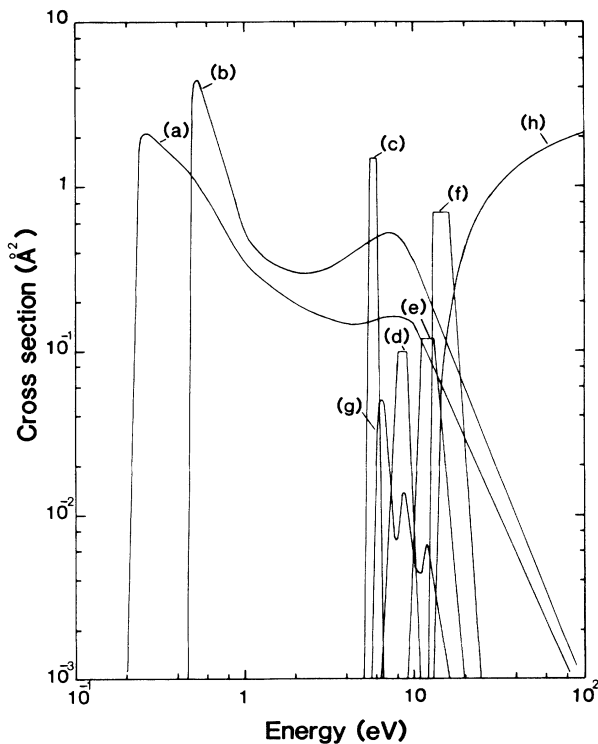
FIG. 2. Total electron-molecule inelastic collision cross sections in water vapor used in the present investigation. (a) and (b) Vibrational cross sections of Seng and Linder (Ref. 10). (c)–(f) Electronic excitation cross sections of Cohen and Phelps (Ref. 22). (g) and (h) attachment and ionization cross section, respectively, of Cohen and Phelps (Ref. 22).
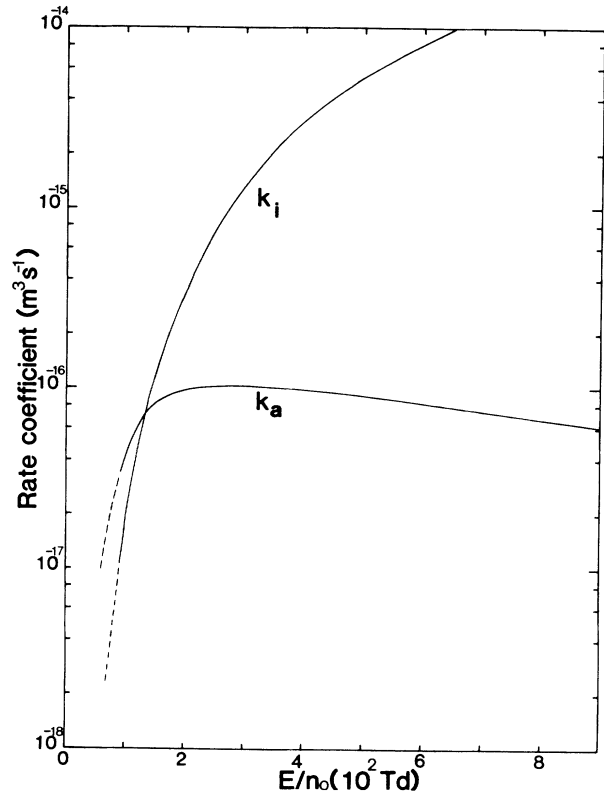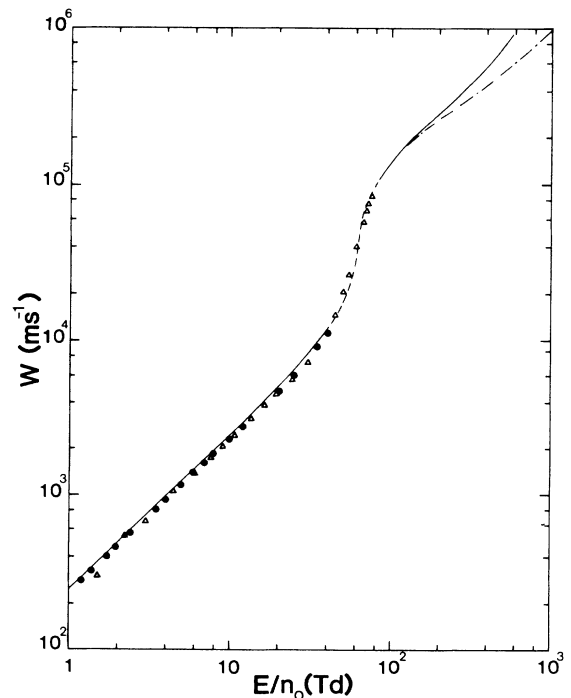
FIG. 4. Drift velocity for electrons in water vapor as a function of E/n_0, $T_0 = 294$ K. Solid curve, present moment calculations; dashed section, interpolation based on partially converged moment solution; ●, experimental values of Lowke and Rees (Ref. 3); △, experimental values of Wilson et al. (Ref. 3); —·—·—·, moment calculations of the coefficient w.
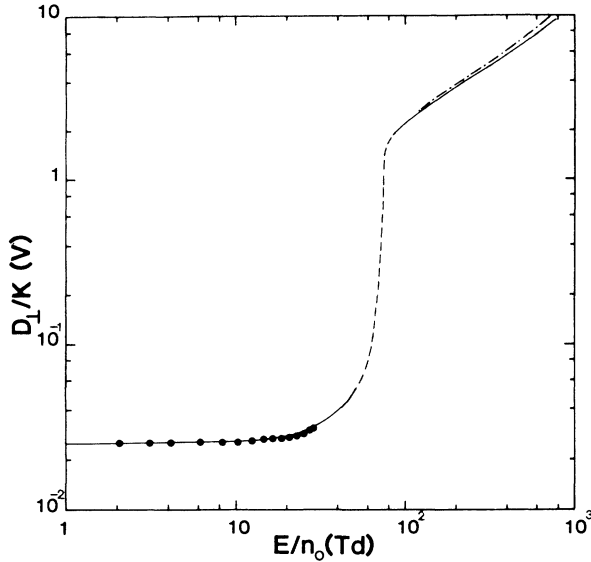
FIG. 5. Ratio of transverse diffusion coefficient to mobility for electrons in water vapor as a function of E/n_0, $T_0 = 294$ K. The solid and the dashed curves have the same meaning as in Fig. 4; ●, experimental values of Elford (Ref. 4); —·—·—·, moment calculations of the quantity $\mathcal{D}_\perp/\mathcal{K}$.

Voshall, and Phelps[2] for $\epsilon < 0.08$ eV with that of Gianturco and Thompson[16] for $\epsilon > 0.08$ eV, as shown in Fig. 1. For rotational interactions the Born approximation results of Itikawa[12] were used. A total of 147 rotational transitions are listed in Table I of Ref. 19. In the present work the largest 100 of these cross sections were used in
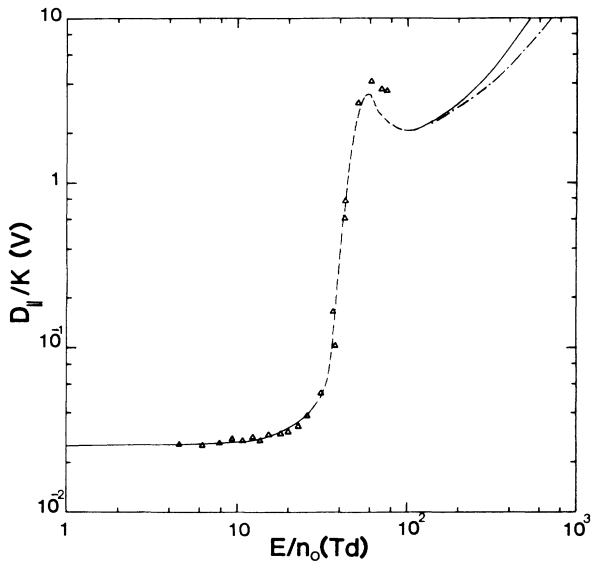

FIG. 6. Ratio of longitudinal diffusion coefficient to mobility for electrons in water vapor as a function of E/n_0, $T_0 = 294$ K. The solid and the dashed curves have the same meaning as in Fig. 4; △, experimental values of Wilson et al. (Ref. 3); —·—·—·, moment calculations of the quantity $\mathcal{D}_\parallel/\mathcal{K}$.

the calculation of the transport coefficients. The addition of further rotational interactions has an insignificant effect upon the transport coefficients.

With the assumption of isotropic scattering, agreement of present calculations with both the measured drift velocities of Lowke and Rees[3] and the measured $D_\perp/K$ values of Elford[4] could not be achieved, even with adjustment of both elastic and rotational cross sections. However, reasonable agreement was obtained by using anisotropic scattering based on the Born approximation for simple charge-dipole interaction.[15,12] For elastic scattering this leads to the following expressions for the quantities $\Delta\sigma_l = \sigma_0 - \sigma_l$:

$$\Delta\sigma_1 = \sigma_0 - \sigma_1 = \sigma_m , \tag{42a}$$

$$\Delta\sigma_2 = \sigma_0 - \sigma_2 = \tfrac{3}{2}\sigma_m , \tag{42b}$$

and for $l \geq 2$,

$$\Delta\sigma_{l+1} = \frac{2l+1}{l+1}\Delta\sigma_l - \frac{l}{l+1}\Delta\sigma_{l-1} , \tag{42c}$$

where

$$\sigma_l(\epsilon) = 2\pi \int_{-1}^{1} \sigma(\epsilon,\chi)P_l(\cos\chi)d(\cos\chi) \tag{43}$$

is the lth partial cross section, $\sigma(\epsilon,\chi)$ is the elastic differential cross section, χ being the center-of-mass (c.m.) scattering angle and σ_m the elastic momentum-transfer cross section, found by subtracting the contribution of inelastic collisions from the total momentum transfer cross section shown in Fig. 1. Equations (42) show that all quantities $\Delta\sigma_l$ which carry the angular dependence of the elastic scattering can be obtained from a knowledge of σ_m.

In the case of rotational interactions, the Born approximation leads to the following expressions for partial cross sections:

$$\sigma_{l,\alpha}^{(\text{rot})}(\epsilon, J\tau \to J'\tau') = \frac{C}{\epsilon} \frac{S_\alpha}{(2J+1)} Q_l(\zeta_\alpha) , \tag{44}$$

$$Q_0(\zeta_\alpha) = \tfrac{1}{4}\ln\left[\frac{\zeta_\alpha+1}{\zeta_\alpha-1}\right] , \tag{45a}$$

$$Q_1(\zeta_\alpha) = \zeta_\alpha Q_0(\zeta_\alpha) - \tfrac{1}{2} , \tag{45b}$$

$$Q_{l+1}(\zeta_\alpha) = \frac{2l+1}{l+1}\zeta_\alpha Q_l(\zeta_\alpha)$$
$$- \frac{l}{l+1}Q_{l-1}(\zeta_\alpha) \ (l \geq 1) , \tag{45c}$$

where the constant C is given by Itikawa[12] as

$$C = \frac{8\pi h^2 D^2}{3m}$$

and D is the dipole moment in atomic units. For water vapor we have taken D to be 0.728 a.u.[12] The quantum numbers $J\tau$ and $J'\tau'$ denote the initial and final rotational states, respectively, J being the angular momentum quantum number and τ being an integer used to designate each of the $2J + 1$ sublevels of a given J.[15] The integer α is an index used in the present work to assign a unique label to each transition. The selection rules for the rota-

tional transitions are discussed in Refs. 12, 15, and 19. The quantity S_α in Eq. (44) denotes the line strength for the transition $J\tau \rightarrow J'\tau'$ and is given in Table I of King, Hainer, and Cross.[19] The variable ζ_α is defined by

$$\zeta_\alpha = \frac{1}{2} \left[\left[\frac{\epsilon}{\epsilon - \epsilon_\alpha} \right]^{1/2} + \left[\frac{\epsilon - \epsilon_\alpha}{\epsilon} \right]^{1/2} \right], \qquad (46)$$

with ϵ_α being the threshold energy for the transition $J\tau \rightarrow J'\tau'$. The energy levels and corresponding relative abundances of rotational states for H_2O can be found in Refs. 21 and 11, respectively. In Ref. 11 the relative abundances of the H_2O rotational states are given for a temperature of 450 K. Using Maxwell-Boltzmann statistics, we have calculated from this data the relative abundance for a temperature of 294 K, used in the present investigation. The three largest $l = 0$ rotational cross sections, weighted by the relative abundance of the lower level in the transition, are shown in Fig. 1. For the 100 rotational transitions considered in the present study the threshold energies range from 0.091 to 40.125 meV.

The vibrational, electronic, attachment, and ionization cross sections used in the present study are shown in Fig. 2. The vibrational cross sections are those of Seng and Linder,[10] while the other cross sections shown in Fig. 2 are those of Cohen and Phelps.[22] For the ionization collision operator[6] the remaining energy after an ionizing collision has been divided equally between the two post-collision electrons. At high values of E/n_0, where ionization is significant, we expect the transport properties to be dependent on how the remaining energy after ionization is partitioned between the two post collision electrons,[6] but this dependence is not studied in the present investigation.

B. Transport coefficients

The transport coefficients along with the mean energy are shown in Figs. 3–7 as functions of E/n_0. The dashed section of these plots in the region 40–90 Td indicates poor convergence of the moment solution. The solid curve represents satisfactory convergence of the transport coefficients to within a few percent or better. The poor convergence of the moment solution corresponds to the region of sharp increase in the transport coefficients and is due to the rapidly falling elastic and rotational cross section for $0.05 \leq \epsilon \leq 2.00$ eV (see Fig. 1). To appreciate why this leads to poor convergence of the moment method we consider an elastic collision model, of the form (11). A two-term analysis[5] for this model gives the following function for the isotropic part of the distribution function:

$$f_0(c) = A(1 + \beta^2 c^2)^{-p}, \qquad (47)$$

where

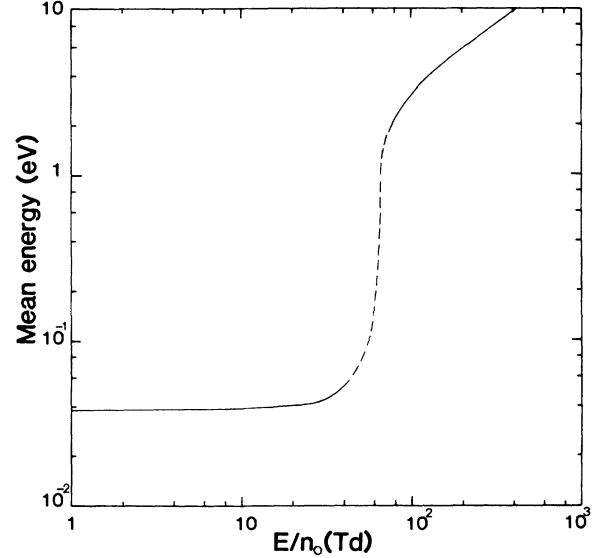$$p = \frac{3}{2} \frac{m}{m_0} \left[\frac{2s_m n_0}{eE} \right]^2 \qquad (48)$$

and

FIG. 7. Mean energy for electrons in water vapor as a function of E/n_0, $T_0 = 294$ K. The dashed section of the curve has the same meaning as in Fig. 4.

$$\beta = \left[\frac{m_0}{3kT_0} \right]^{1/2} \frac{eE}{2n_0 s_m}. \qquad (49)$$

Moments of f_0 arise in the form

$$\int_0^\infty c^2 f_0(c) c^n dc = \int_0^\infty \frac{c^{2+n}}{(1 + \beta^2 c^2)^p} dc. \qquad (50)$$

This integral exists only if

$$p > \frac{3+n}{2},$$

i.e.,

$$\frac{E}{n_0} < \left[\frac{m}{m_0} \right]^{1/2} \left[\frac{2s_m}{e} \right] \left[\frac{3}{3+n} \right]^{1/2} = \left[\frac{E}{n_0} \right]_{\text{critical}}. \qquad (51)$$

Thus we see that above a certain critical value of E/n_0, moments of the distribution function for this particular model of interaction do not exist. Setting $n = 0$ in expression (51) gives the same critical value of fields as condition (37) of Sec. II C 1. Note also that the larger n is, i.e., the higher the moment, the smaller the critical value of E/n_0. Thus, in the vicinity of the critical field for a given transport coefficient, increasing the order of approximation, i.e., increasing the number of Sonine polynomials in the moment expansion beyond a certain point is of no use and leads to divergence rather than convergence.[23] In the case of electrons in water vapor we observe this type of behavior in the region 40–90 Td where the mean energy ranges from 0.05 to 2 eV (see Fig. 7), σ_m is decreasing as approximately ϵ^{-1}, and the rotational cross sections of Itikawa are also rather sharply decreasing functions of ϵ. This leads to the quasirunaway effect discussed in Sec. II C 2 resulting in a strongly non-Maxwellian distribution and hence poor convergence for the present moment solution. As E/n_0 increases above

90 Td, ϵ increases above 2 eV, the momentum-transfer cross section levels off, and the higher-order inelastic processes (including attachment and ionization) become important. The effect of this is to improve the thermal contact between electrons and water-vapor molecules, making the electron distribution closer to Maxwellian and thus re-establishing satisfactory convergence of the moment method.

In Fig. 3 we show the ionization rate coefficient $k_i = \bar{v}_i / n_0$ and the attachment rate coefficient $k_a = \bar{v}_a / n_0$ versus E / n_0, where $\bar{v}_i$ and $\bar{v}_a$ denote the swarm average ionization and attachment frequency, respectively. The two rate coefficients cross at approximately 140 Td, indicating that the production of free electrons by ionization dominates the loss of electrons by attachment for $E / n_0 \geq 140$ Td. In the solution of the first set of our moment equations, i.e., the eigenvalue problem,[6] this corresponds to the dominant eigenvalue changing sign from negative to positive. Note that in Fig. 3 for $E / n_0 < 100$ Td the onset of attachment is rapid as predicted by the momentum transfer theory of Sec. II C 2.

The average ionization and attachment frequencies are related to the ionization and attachment coefficients α and η, respectively, as measured in steady-state Townsend experiments, by

$$\bar{v}_i \simeq \alpha W \ ,$$

$$\bar{v}_a \simeq \eta W \ .$$

Here we stress that these are only approximate relationships and the connection between transport coefficients and experimental arrangement is a matter under current investigation. We intend to solve a more general eigenvalue problem appropriate to both time of flight and steady-state Townsend experiments, but leave this to a future publication.

The center-of-mass drift velocity along with the experimental results of Lowke and Rees[3] and Wilson et $al.$[3] are shown in Fig. 4. We see that the present calculations of W tend to lie a little above the experimental results; nevertheless, the agreement is still quite reasonable. The ratios $D_\perp / K$ and $D_\parallel / K$ are shown in Figs. 5 and 6, where they are compared to the experimental results of Elford[4] and Wilson et $al.$,[3] respectively. Here the agreement is good, particularly in the low E / n_0 range which lends support to the Itikawa rotational cross sections. We point out that theoretical calculations of electrons transport coefficients in water vapor have also been carried out by Lowke and Parker,[8] using the two-term approximation, and by Yousfi et $al.$[7] using a multiterm theory, but as a different set of cross sections has been used in all three cases, no direct comparison between the theoretical results is made. Nevertheless, the transport coefficients as a function of E / n_0 show the same behavior qualitatively. There is, however, some difference in the detail, in particular, the agreement between the present theory and experiment for $D_\perp / K$ and $D_\parallel / K$ in the low E / n_0 range $(E / n_0 < 30$ Td) is somewhat better than that for Yousfi et $al.$[7] This indicates that the Itikawa rotational cross sections are a better approximation than the total rotational cross section used by Yousfi et $al.$[7] In the present

investigation attempts were made at modeling the rotational interactions by a single cross section, but this proved unsuccessful in fitting the $D_\perp / K$ data of Elford[4] over the entire experimental range of E / n_0.

The plot of mean energy shown in Fig. 7 confirms the momentum-transfer analysis of Sec. II. Note that the average swarm energy remains near thermal over a rather large range of E / n_0 (0–25 Td). This strong thermalization effect of water vapor on electrons is due to the large number of low-threshold-energy-rotational transitions and not the momentum-transfer cross section, as suggested by Lowke and Parker.[8] The analysis in Sec. II C 1 predicts that without the rotational interactions the mean energy would be near thermal for only a few townsend, a prediction that is readily varified by solving the Boltzmann equation for low E / n_0 without the rotational transitions.

Also shown in Figs. 4, 5, and 6 are the coefficients ω, $\mathcal{D}_\perp / \mathcal{K}$, and $\mathcal{D}_\parallel / \mathcal{K}$, respectively. In the context of a Boltzmann-equation solution these coefficients have been defined earlier[24] and they give the value of the transport excluding the explicit effect of reactions. From these plots it is evident that the difference between W and w, $D_\perp$ and $\mathcal{D}_\perp$, and $D_\parallel$ and $\mathcal{D}_\parallel$ only become important at high-field strengths where the production of electrons by ionization dominates the reactive process. Note that at these high-field strengths $W > w$, $D_\perp / K < \mathcal{D}_\perp / \mathcal{K}$, and $D_\parallel / K > \mathcal{D}_\parallel / \mathcal{K}$, which confirms the analysis of Sec. II C 3. In the case of W, the greater ionization rate by the more energetic electrons at the front of the swarm enhances the center-of-mass drift velocity, hence $W > w$. For intermediate fields, where attachment is the dominant reactive process, the analysis of Sec. II C 2 predicts that $W < w$, but the difference is very small. In our Boltzmann-equation solution, we find this to be the case with the difference between W and w being of the order of 0.1% and less. For the intermediate field strengths the attachment of the more energetic electrons at the front of the swarm retards the centroid velocity, hence $W < w$. However, this effect is significantly reduced by the large inelastic processes in the vicinity of attachment (see Fig. 2). If one repeats the analysis of Sec. II C 2, omitting the electronic excitation process, then a significant difference between W and w is found, with $\delta_W = 0.186$.

Finally, in Fig. 8 we show the percentage difference between multiterm results and the two-term approximation for the transport coefficients as a function of E / n_0. For low-field strengths the two-term approximation is quite adequate, however, it clearly becomes less accurate at higher-field strengths. For $D_\parallel$ in Fig. 8 we have plotted half the percentage difference, so that at 1000 Td the difference between the two-term approximation and the converged multiterm results for $D_\parallel$ is almost 50%. Up to six terms were considered in the spherical harmonic expansion, but for the range of E / n_0 considered satisfactory convergence was achieved after four terms.

IV. CONCLUDING REMARKS

We have attempted to understand the transport properties of electrons in water vapor (a) physically, using the
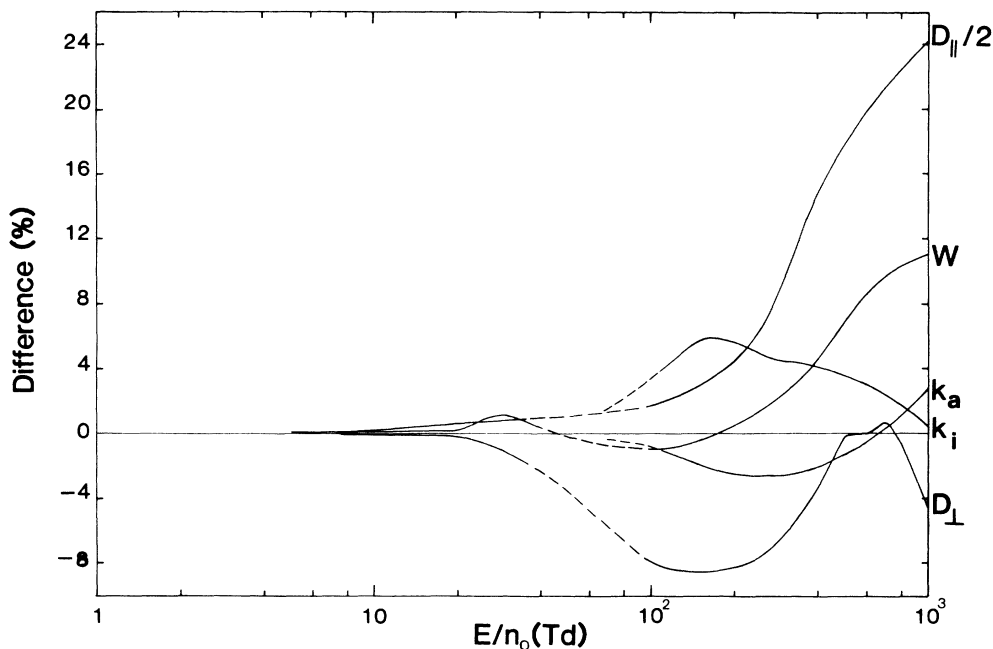
FIG. 8. Percentage difference between multiterm and two-term results of transport coefficients for electrons in water vapor as a function of E/n_0, $T_0 = 294$ K. The dashed section of the curves has the same meaning as in Fig. 4. Negative numbers indicate that the two-term result is larger.

momentum-transfer theory and, (b) quantitatively, using the best available estimates of cross sections, coupled with up-to-date experimental data and a sophisticated moment method of solution of Boltzmann's equation. As has been pointed out earlier by Gallagher et al.[1] the behavior of electrons in water vapor is characterized by three regions of E/n_0. The present work clearly confirms this. The main results are as follows.

(1) In the region below 30 Td the electrons remain essentially thermal with their behavior being dominated by the large number of low-threshold energy rotational transitions. In this region we obtain good agreement between experiment and theory, particularly for the $D_\perp/K$ values by using the Born-approximation rotational cross sections of Itikawa[12] and incorporating anisotropic scattering into our calculations.

(2) In the intermediate region between 30 and 90 Td the electron swarm behavior is strongly influenced by the rapidly falling elastic and rotational cross sections for energies between 0.04 and 2 eV and as a consequence all transport coefficients show a rapid increase with E/n_0. We have referred to this as quasirunaway behavior, and, due to the limitations of Burnett function expansions with a Gaussian weight function, the moment method gave less than satisfactory convergence for $40 < E/n_0 < 90$ Td. Thus in this region, a modification of the present two-temperature moment method or a different numerical approach will be required for precise computation of transport coefficients.

(3) For E/n_0 above 90 Td the combined effect of the higher-threshold inelastic processes (electronic excitation, attachment, and ionization) on the swarm becomes significant and the tendency to runaway is quenched with the transport coefficients settling down to a somewhat slower variation with E/n_0.

It is hoped that the present study will provide incentive for both further theoretical and experimental investigations of this most important of substance.

ACKNOWLEDGMENTS

[1]J. W. Gallagher, E. C. Beaty, J. Dutton, and L. C. Pitchford, J. Phys. Chem. Ref. Data 12, 109 (1983).

[2]J. L. Pack, R. E. Voshall, and A. V. Phelps, Phys. Rev. 127, 2084 (1962).

[3]J. J. Lowke and J. A. Rees, Aust. J. Phys. 16, 447 (1963); H. Ryzko, Proc. Phys. Soc. 85, 1283 (1965); H. Ryzko, Ark. Fys. 32, 1 (1966); R. W. Crompton, J. A. Rees, and R. L. Jory, Aust. J. Phys. 18, 541 (1965); J. F. Wilson, F. J. Davis, D. R.

Nelson, R. N. Compton, and O. H. Crawford, J. Chem. Phys. **62**, 4204 (1975).

[4]M. T. Elford, in *Proceedings of the XVIII International Conference on the Phenomena in Ionized Gases, Swansea, Wales*, edited by W. T. Williams (Hilger, London, 1987), p. 130.

[5]L. G. H. Huxley and R. W. Crompton, *The Diffusion and Drift of Electrons in Gases* (Wiley, New York, 1974).

[6]R. E. Robson and K. F. Ness, Phys. Rev. A **33**, 2068 (1986); K. F. Ness and R. E. Robson, *ibid.* **34**, 2185 (1986).

[7]M. Yousfi, P. Segur, and T. Vassiliadis, J. Phys. D **18**, 359 (1985). Yousfi and co-workers have also compiled data on cross sections and swarm parameters for several atomospheric gases, including water vapor (unpublished).

[8]J. J. Lowke and J. H. Parker, Phys. Rev. **181**, 302 (1969).

[9]R. E. Robson, J. Phys. Chem. **85**, 4486 (1986).

[10]G. Seng and F. Linder, J. Phys. B **9**, 2539 (1976).

[11]K. Jung, T. Antoni, R. Muller, K.-H. Kochem, and H. Ehrhardt, J. Phys. B **15**, 3535 (1982).

[12]Y. Itikawa, J. Phys. Soc. Jpn. **32**, 217 (1972).

[13]Y. Itikawa, J. Phys. Soc. Jpn. **36**, 1121 (1974); **36**, 1127 (1974).

[14]S. Altshuler, Phys. Rev. **107**, 114 (1957).

[15]O. H. Crawford, J. Chem. Phys. **47**, 1100 (1967).

[16]F. A. Gianturco and D. G. Thompson, J. Phys. B **13**, 613 (1980).

[17]J. J. Olivero, R. W. Stagat, and A. E. S. Green, J. Geophys. Res. **77**, 4797 (1972).

[18]D. W. Norcross, in *Applied Atomic Collision Physics*, edited by H. S. W. Massey, E. W. McDaniel, and B. Bedersen (Academic, New York, 1982), Vol. 5, p. 69.

[19]G. W. King, R. M. Hainer, and P. C. Cross, Phys. Rev. **71**, 433 (1947).

[20]R. E. Robson, Aust. J. Phys. **37**, 35 (1984).

[21]R. T. Hall and J. M. Dowling, J. Chem. Phys. **47**, 2454 (1967).

[22]J. J. Lowke (private communication).

[23]H. R. Skullerud, J. Phys. B **17**, 913 (1984).

[24]These coefficients are defined in Ref. 6 above, where the symbols used to denote them are W^*, $D_\perp^*$ and $D_\parallel^*$.